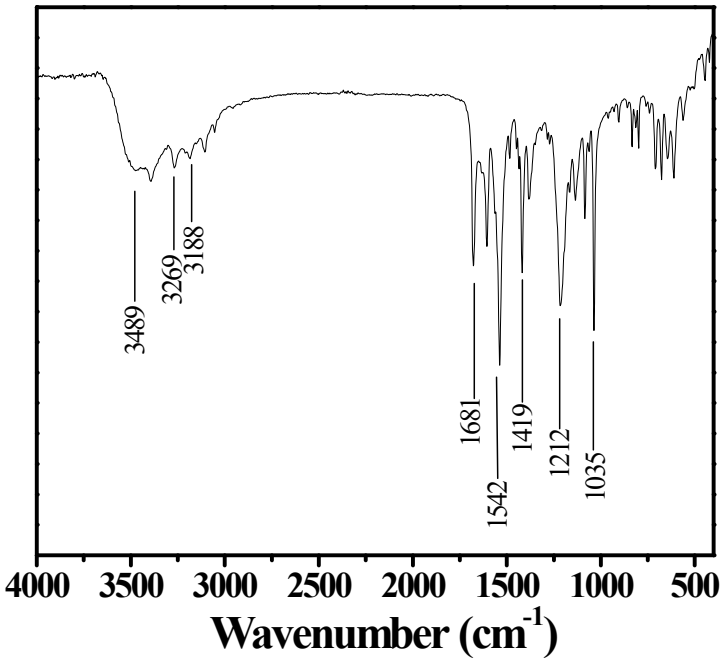

Fig. S1. The FT-IR spectrum of **1**.

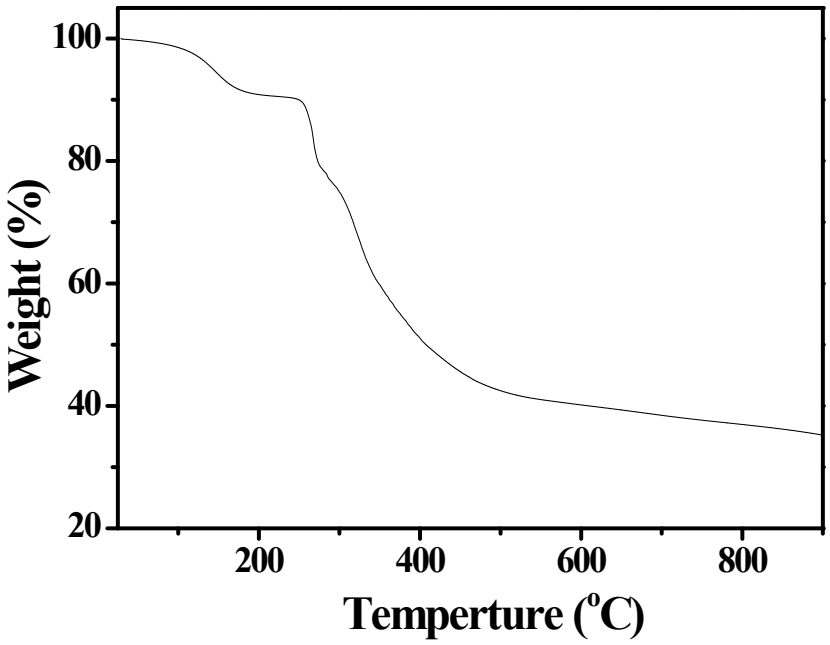

Fig. S2. The thermogravimetric analysis (TGA) curve of **1**.

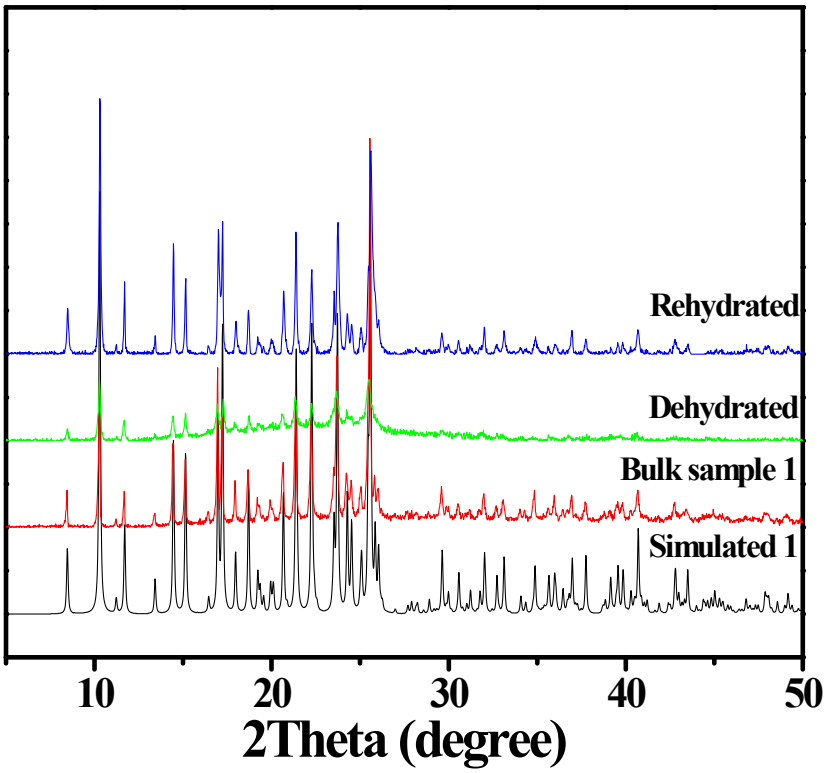

Fig. S3. The VT–PXRD patterns for **1**, showing the simulated XRD pattern calculated from single-crystal X-ray diffraction data with Mercury (black), the bulk sample of **1** (red), after removal of the water molecules at 473 K (green) and after being exposed in water vapour for about one week at room temperature (blue).

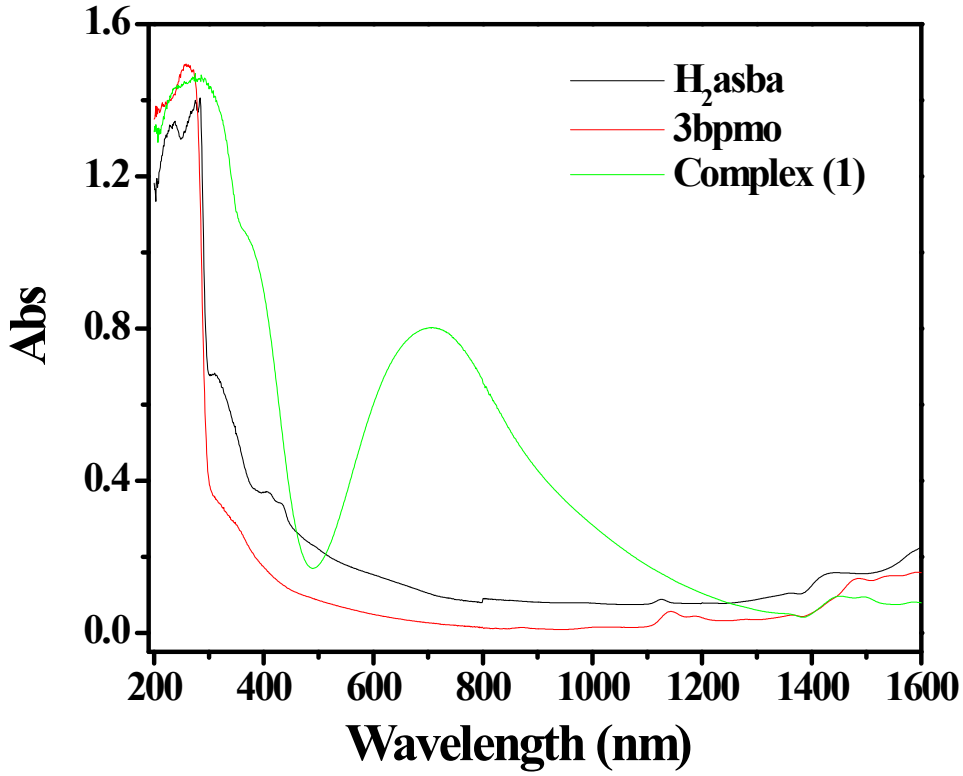

Fig. S4. The solid-state UV–Vis–NIR spectra for **1** (green), H_2asba (black) and 3bpmo (red), respectively.

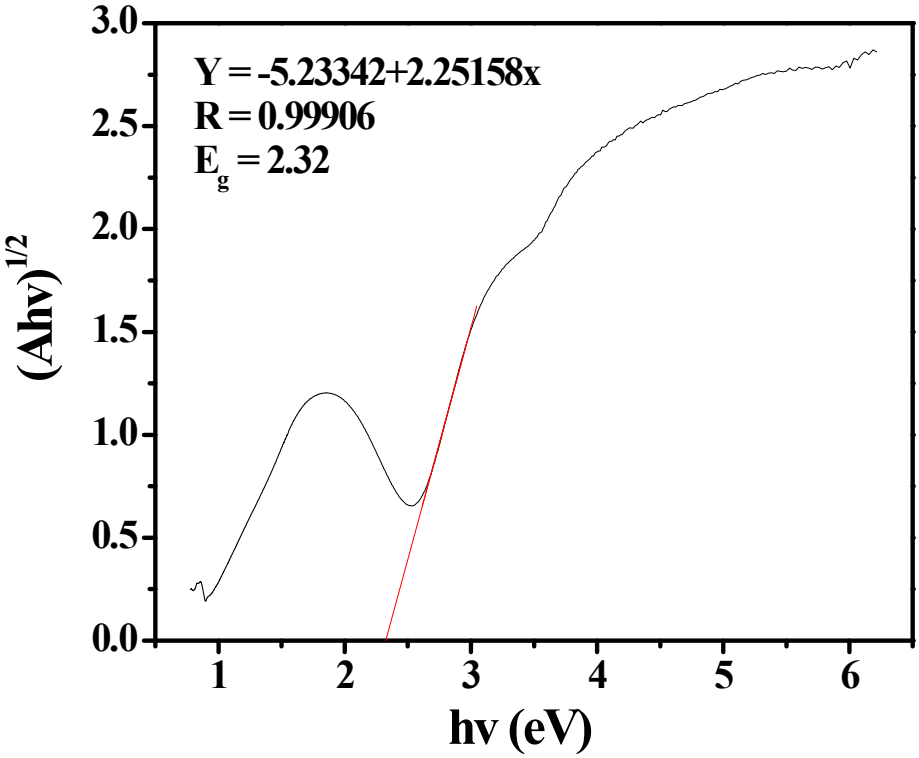

Fig. S5. The solid-state diffuse reflectance UV-Vis-NIR spectrum of $(Ah\nu)^{1/2}$ *versus* hν (eV) for **1**.

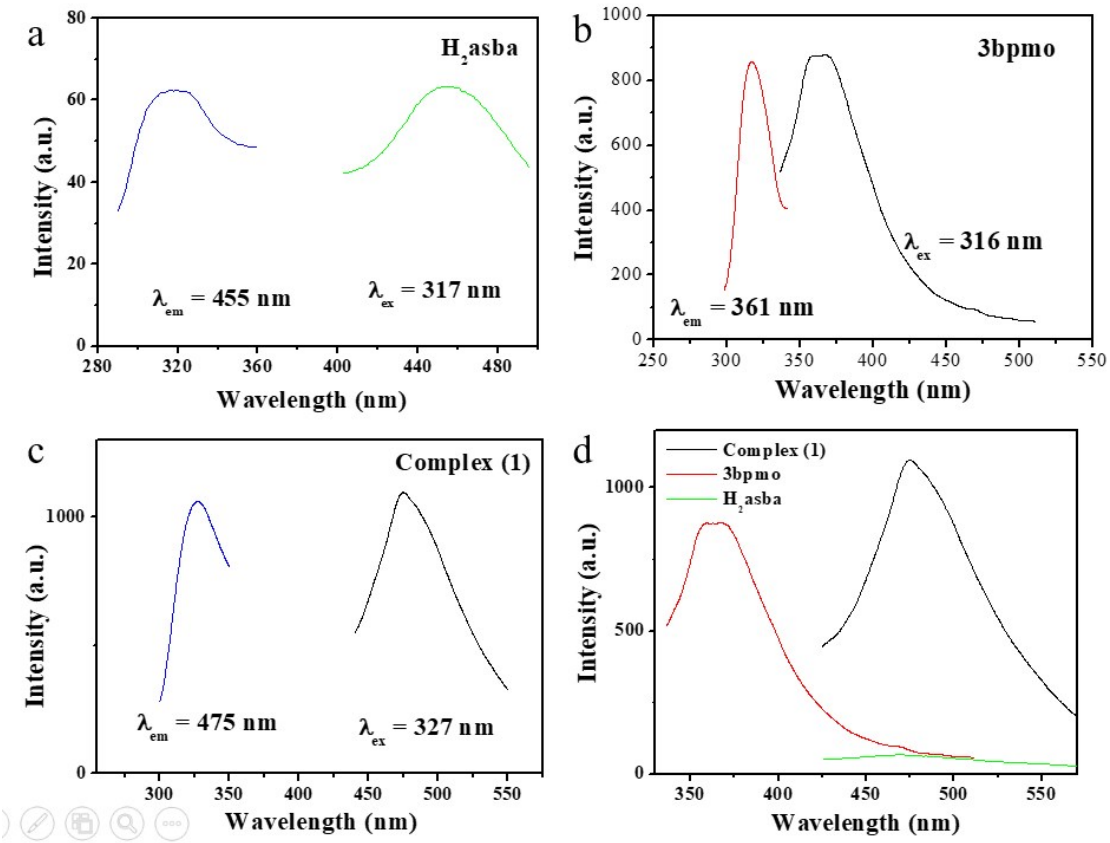

Fig. S6. Excitation (blue) and emission spectra of (**a**) H_2asba (λ_{ex} = 317 nm), (**b**) 3bpmo (λ_{ex} = 316 nm), (**c**) MOF **1** (λ_{ex} = 327 nm), and (**d**) a comparison of the solid-state fluorescence emission spectra of **1** (black), 3bpmo (red) and H_2asba (green), respectively.

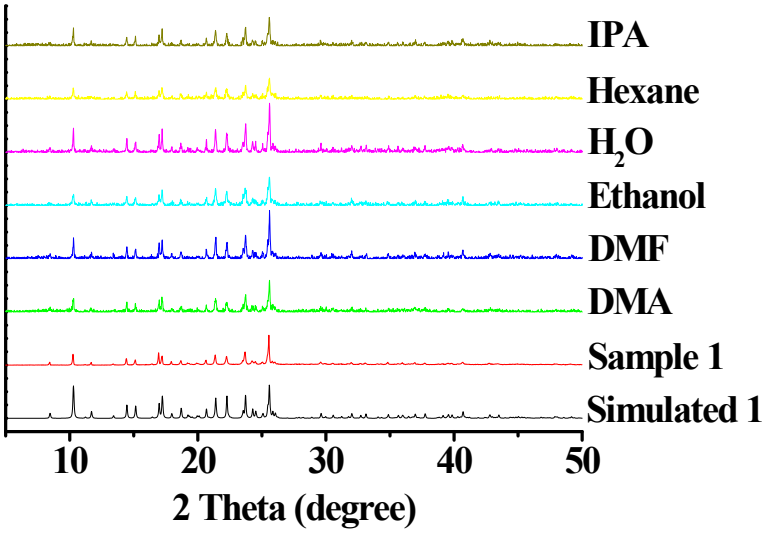

Fig. S7. The PXRD patterns of **1** after being immersed in various solvents.

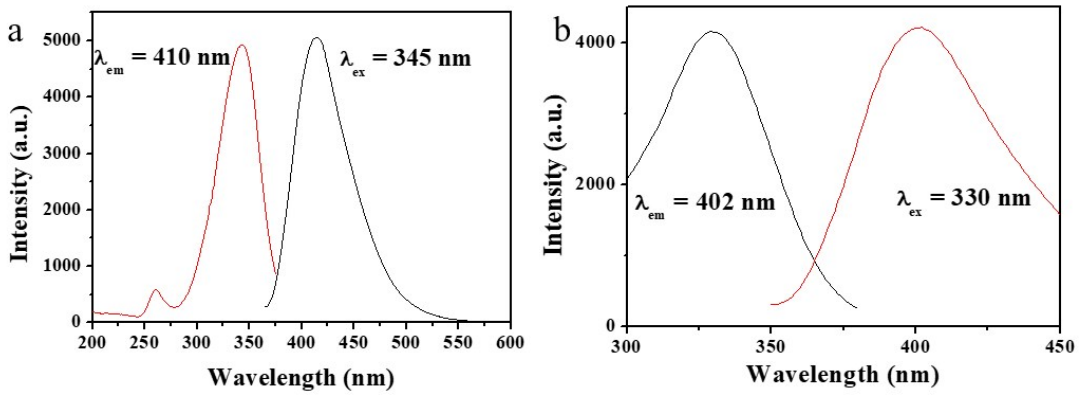

Fig. S8. The excitation and emission spectra of **1** in DMF **(a)** and water **(b)**, respectively.

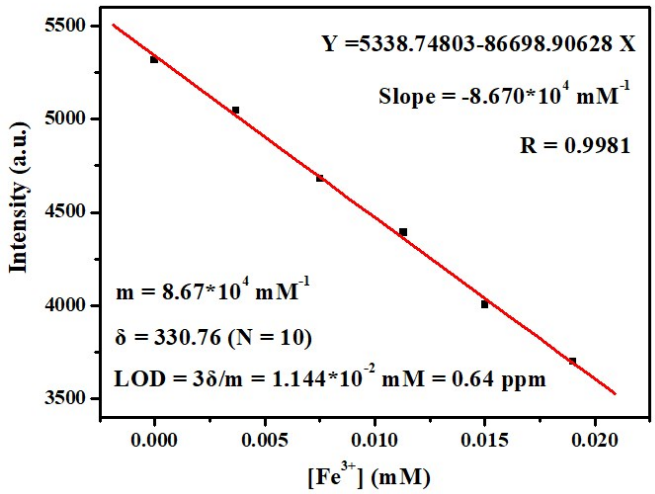

Fig. S9. The fitting curve of the luminescence intensity of **1** at different Fe^{3+} concentrations in DMF (linear range 0 - 0.01875 mM).

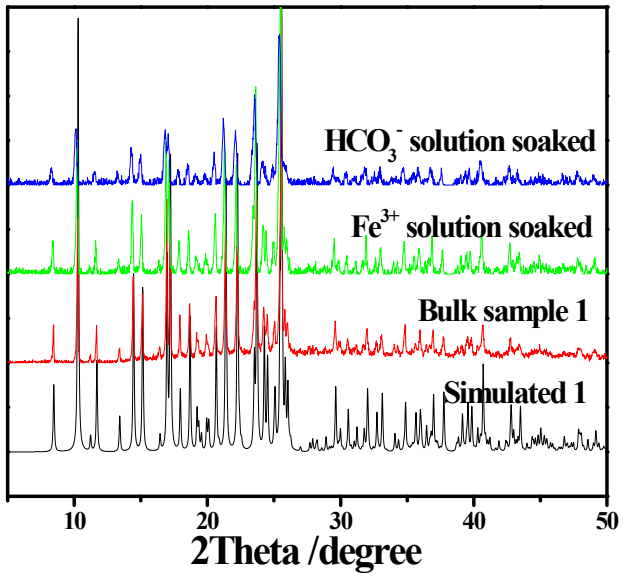

Fig.S10. PXRD patterns of **1** after being soaked in the mixed DMF-H_2O solution of Fe^{3+}/HCO_3^- [0.225 mM, V(DMF:H_2O) = 1000:1] for about 1 day.

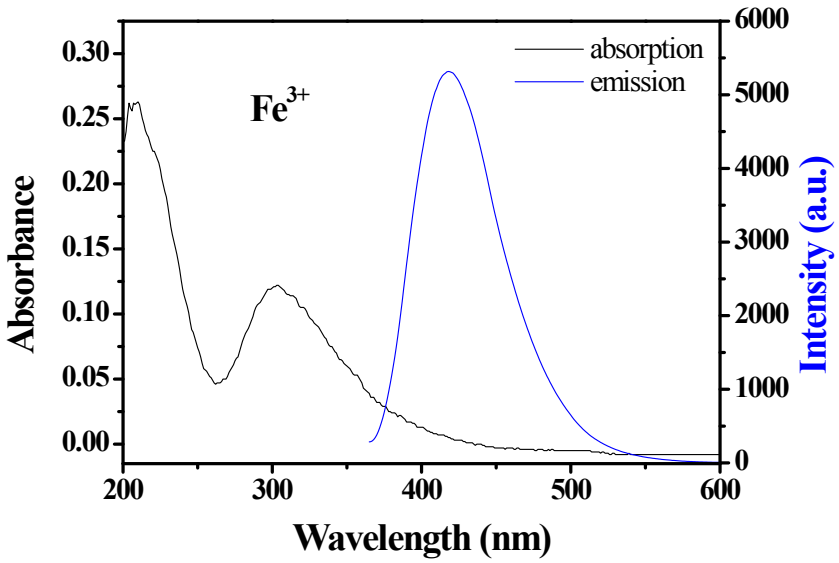

Fig. S11. The spectral overlap between the absorption spectrum of Fe^{3+} (7.5×10^{-5} mol/L) in DMF (Fe^{3+} aqueous solution : DMF = 1:1000) and the fluorescence emission spectrum of the DMF suspension of **1** (λ_{ex} = 345 nm).

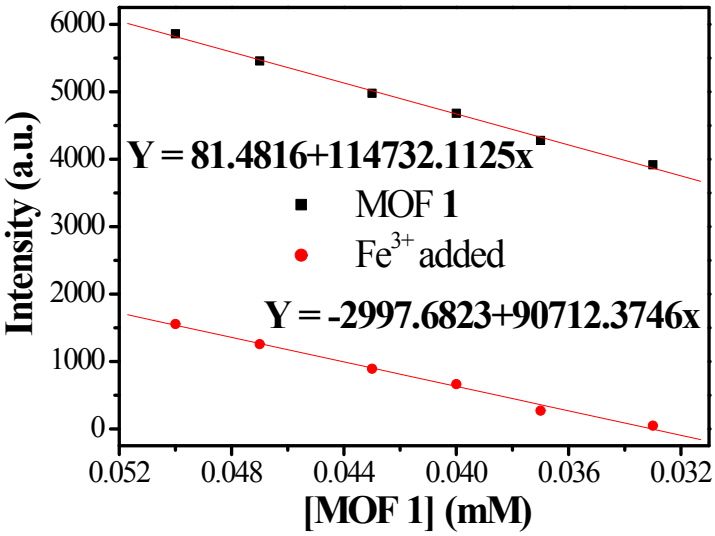

Figure S12. The best-linear fitting of the fluorescence intensity of the DMF suspensions of **1** *versus* the concentration of **1** (0.05 mM – 0.033 mM) before and after the addition of Fe^{3+} (0.075 mM), respectively.

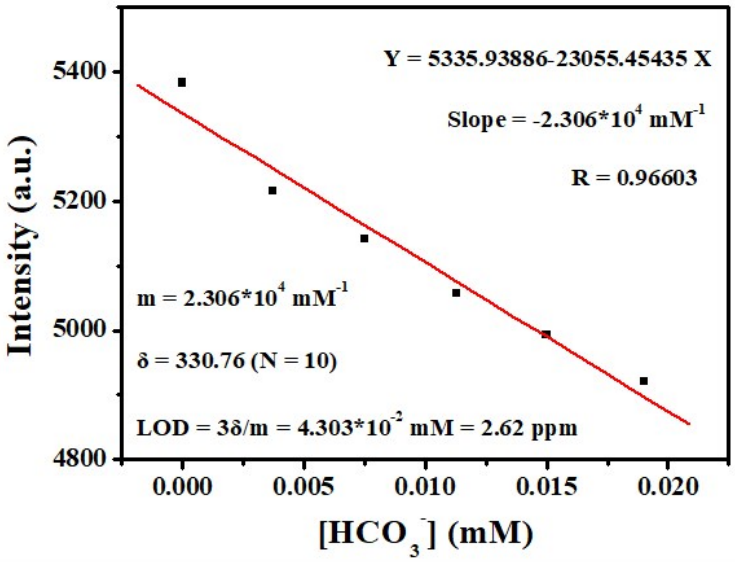

Fig. S13. The fitting curve of the luminescence intensity of **1** at different HCO_3^- concentrations in DMF (linear range 0 - 0.01875 mM).

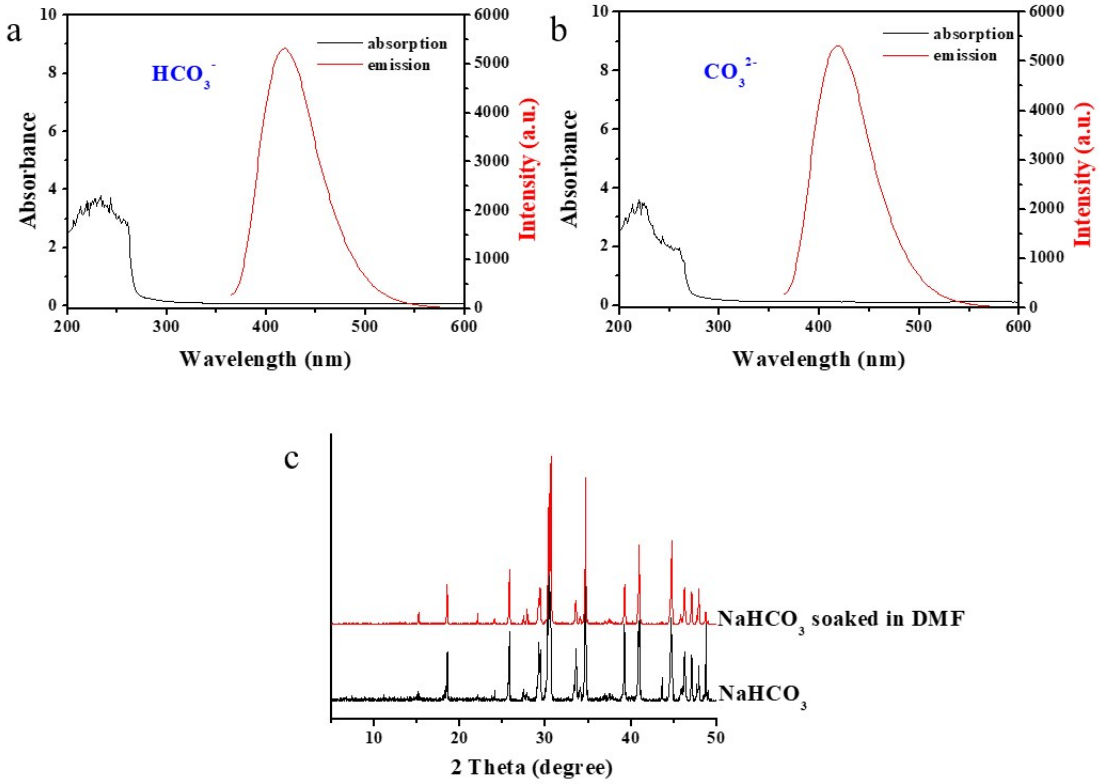

Fig. S14. (a) Absorption spectrum of HCO_3^- in DMF (7.5×10^{-5} mol/L) and fluorescence emission spectrum of **1** (λ_{ex} = 345 nm). (b) Absorption spectrum of CO_3^{2-} in DMF (7.5×10^{-5} mol/L) and emission spectrum of **1** (λ_{ex} = 345 nm). (c) The PXRD pattern of $NaHCO_3$ after being soaked in DMF for about 1 day, revealing $NaHCO_3$ shows high stability in DMF.

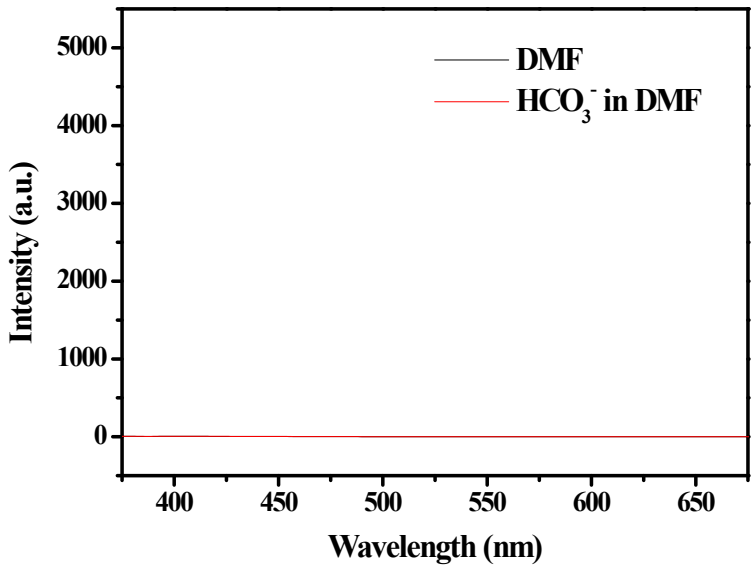

Fig. S15. Fluorescence emission spectra of HCO_3^- (7.5×10^{-5} mol/L) in DMF (λ_{ex} = 345 nm).

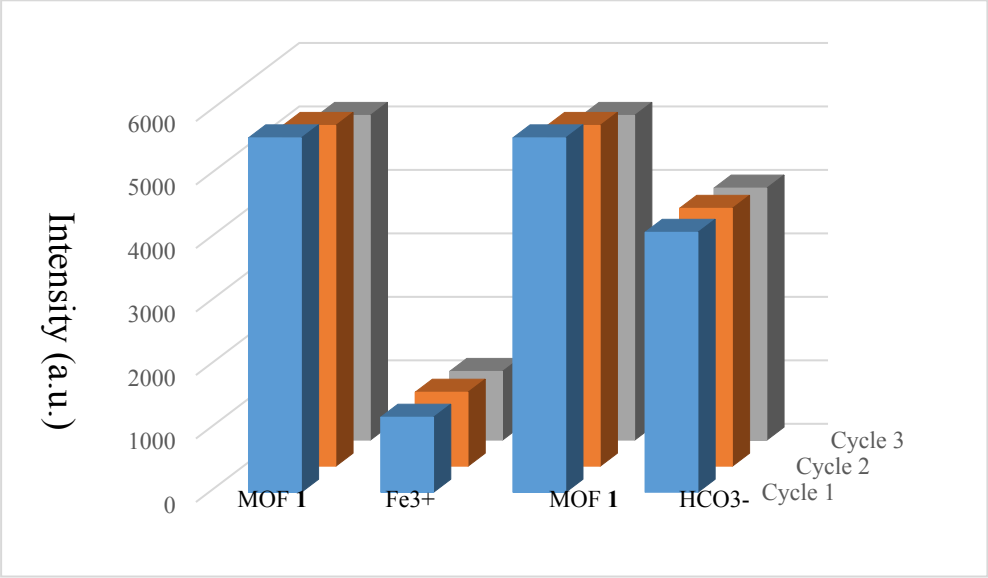

Fig. S16. The fluorescence emission intensity of the DMF suspensions of **1** before and after addition of Fe^{3+} (0.225 mM) and HCO_3^- (0.225 mM) during three cycles**.**

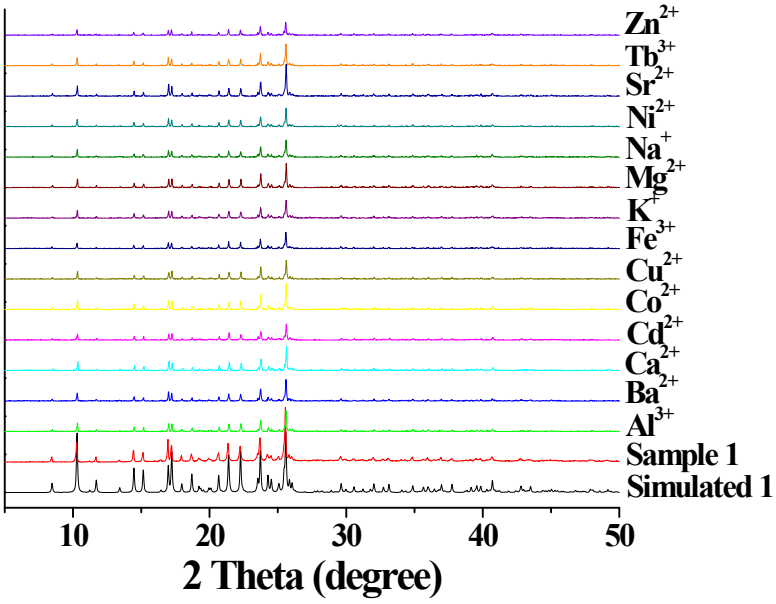

(a)

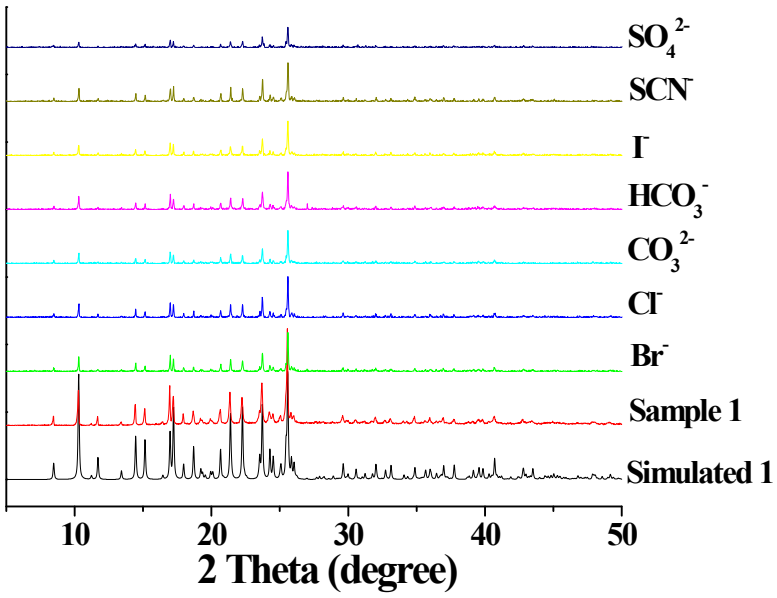

(b)

Fig. S17. The PXRD patterns of **1** after being immersed in each of aqueous ion solutions: (a) metal ions, (b) anions.

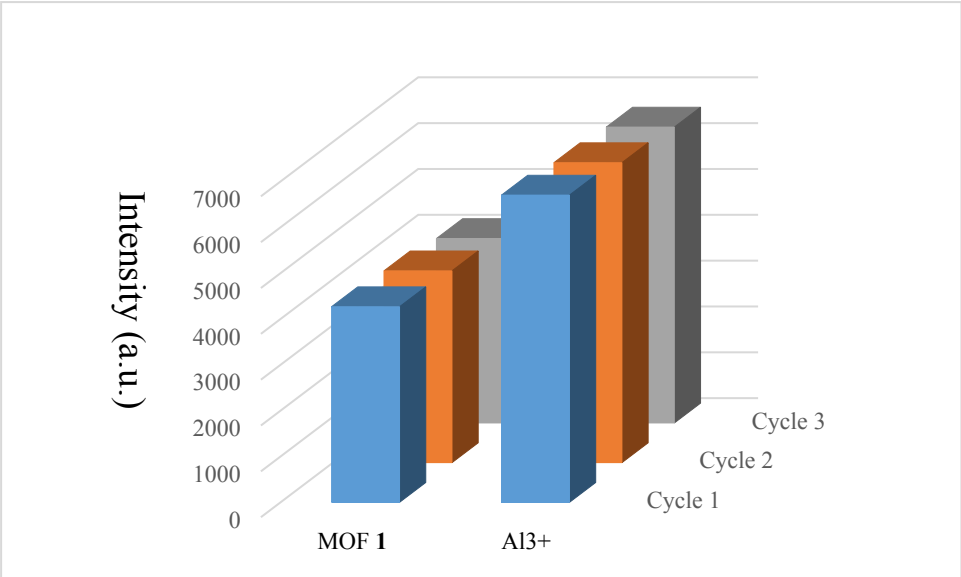

Fig. S18. The fluorescence emission intensity of the aqueous suspensions of **1** before and after addition of Al^{3+} (0.225 mM) during three cycles.

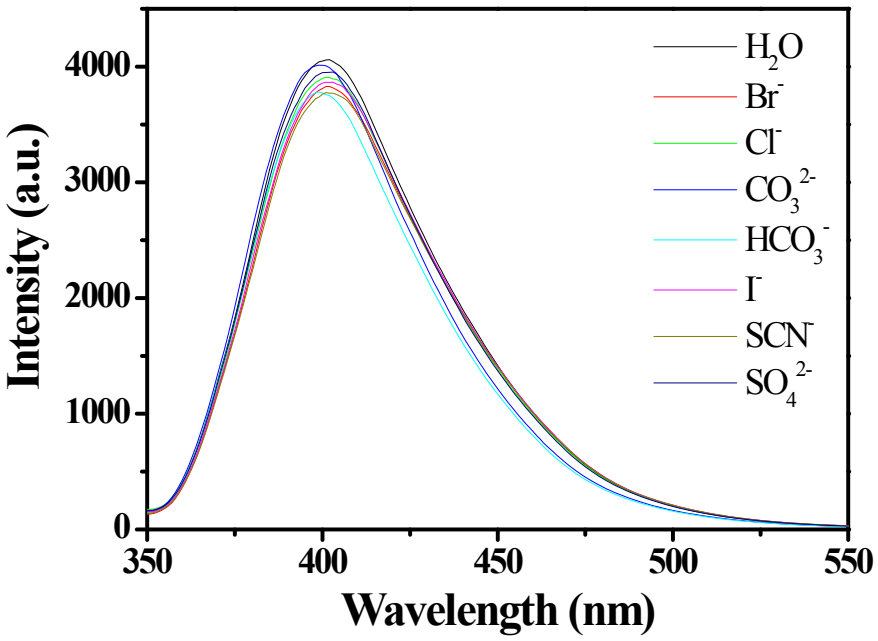

Fig. S19. Fluorescence spectra of **1** (2.0 ml, 5 × 10^{-5} mol/L) with each of the anions (0.075 mmol/L) in water (λ_{ex} = 330 nm).

Table S1 Selected geometric parameters (Å, º) for (**1**)

Cu1—O2^{i}	1.9787 (16)	Cu1—N1	2.0114 (19)
Cu1—O1	1.9796 (17)	Cu—O1W	2.2610 (19)
Cu1—N3	1.981 (2)		
O2^{i}—Cu1—O1	169.18 (8)	N3—Cu1—N1	166.12 (9)
O2^{i}—Cu1—N3	90.76 (8)	O2^{i}—Cu1—O1W	99.68 (8)
O1—Cu1—N3	91.20 (8)	O1—Cu1—O1W	90.63 (8)
O2^{i}—Cu1—N1	87.76 (7)	N3—Cu1—O1W	97.35 (9)
O1—Cu1—N1	87.80 (7)	N1—Cu1—O1W	96.50 (9)

Symmetry codes: (i) $-x+1/2, y-1/2, z$; (ii) $-x+1/2, y+1/2, z$.

Table S2 Hydrogen-bond geometry (Å, º) for (1)

D—H···*A*	*D*—H	H···*A*	*D*···*A*	*D*—H···*A*
O1*W*—H1*WB*···O2*W*^{iii}	0.84	1.94	2.757 (3)	162
O1*W*—H1*WA*···O6^{iv}	0.84	2.16	2.933 (3)	153
N2—H2*A*···O6^{v}	0.86	2.31	2.691 (3)	107
N2—H2*A*···O1*W*^{vi}	0.86	2.56	3.414 (3)	170
O2*W*—H2*WA*···O3^{vi}	0.85	2.39	3.033 (4)	133
O2*W*—H2*WA*···O4^{vi}	0.85	2.20	3.009 (4)	158
Cu1—H3*A*···O5^{vi}	1.33	2.28	3.004 (3)	110
N3—H3*B*···O1^{i}	0.86	2.38	3.039 (3)	134
O2*W*—H2*WB*···O3^{vii}	0.85	2.11	2.901 (4)	155
O2*W*—H2*WB*···O6^{viii}	0.85	2.54	3.023 (3)	117
C8—H8···O2*W*^{ix}	0.93	2.53	3.408 (4)	158

Symmetry codes: (i) −*x*+1/2, *y*−1/2, *z*; (ii) −*x*+1/2, *y*+1/2, *z*; (iii) −*x*+1/2, −*y*+1, *z*−1/2; (iv) *x*+1/2, −*y*+3/2, −*z*; (v) −*x*, −*y*+2, −*z*; (vi) *x*−1/2, *y*, −*z*+1/2; (vii) −*x*+1, *y*+1/2, −*z*+1/2; (viii) *x*+1/2, *y*, −*z*+1/2; (ix) *x*, −*y*+3/2, *z*−1/2.

Table S3 The relative quantum yields of **1** in different solvents

DMA	DMF	EtOH	H_2O	IPA	Hexane
0.106	0.384	0.017	0.117	0.102	0.003